PROCEEDINGS OF SCIENCE

ONLINE ICRC 2021
THE ASTROPARTICLE PHYSICS CONFERENCE
Berlin | Germany
37th International Cosmic Ray Conference
12–23 July 2021

New cosmic ray MIN-MED-MAX benchmark models for dark matter indirect signatures

Pierre Salati,[a,*] **Mathieu Boudaud,**[b] **Marco Cirelli,**[c] **Laurent Derome,**[d] **Yoann Génolini,**[e] **Julien Lavalle,**[f] **David Maurin**[d] **and Pasquale Dario Serpico**[a]

[a] *LAPTh, Université Savoie Mont Blanc & CNRS, Chemin de Bellevue, 74941 Annecy Cedex, France*
[b] *Instituto de Física Teórica UAM/CSIC, Calle Nicolás Cabrera 13-15, Cantoblanco E-28049 Madrid, Spain*
[c] *LPTHE, CNRS & Sorbonne University, 4 place Jussieu, 75252 Paris Cedex 05, France*
[d] *LPSC, Université Grenoble Alpes & CNRS/IN2P3, 53 avenue des Martyrs, 38026 Grenoble, France*
[e] *Niels Bohr International Academy & Discovery Center, Niels Bohr Institute, University of Copenhagen, Blegdamsvej 17, DK-2100 Copenhagen, Denmark*
[f] *LUPM, CNRS & Université de Montpellier, Place Eugène Bataillon, 34095 Montpellier Cedex 05, France*
E-mail: pierre.salati@lapth.cnrs.fr, Deceased, marco.cirelli@gmail.com, laurent.derome@lpsc.in2p3.fr, Yoann.Genolini@nbi.ku.dk, lavalle@in2p3.fr, david.maurin@lpsc.in2p3.fr, serpico@lapth.cnrs.fr

Galactic charged cosmic rays, notably positrons, antiprotons and light antinuclei, are powerful probes of dark matter annihilation or decay, in particular for candidates heavier than a few MeV or tiny evaporating primordial black holes. Recent measurements by PAMELA, AMS-02, or Voyager on positrons and antiprotons already translate into constraints on several models over a large mass range. However, these constraints depend on Galactic transport models, in particular the diffusive halo size L, subject to theoretical and statistical uncertainties. Using Be/B data on top of the secondary-to-primary ratios Li/C and B/C, we have set new constraints on L. We have derived an average value of $L = 5^{+3}_{-2}$ kpc at 1σ. These constraints improve by a factor of 2 when low-energy ^{10}Be/Be and ^{10}Be/^{9}Be data are included.

Using these results, we have updated the so-called MIN-MED-MAX benchmark transport parameters that yield generic minimal, median, and maximal dark matter produced fluxes. We define these benchmark configurations from a selection of models based on the diffusive halo height L and on a specific low-energy transport parameter that depends on the cosmic-ray transport scheme. We illustrate our results with a 100 GeV dark matter species annihilating into $b\bar{b}$ quark or electron-positron pairs, and present the positron and antiproton fluxes that these particles generate at the Earth. With our revised MIN-MED-MAX benchmarks, the uncertainties on primary fluxes reduce by a factor of 3-4 (positrons) and 5 (antiprotons) with respect to their former version.

37th International Cosmic Ray Conference (ICRC 2021)
July 12th – 23rd, 2021
Online – Berlin, Germany

*Presenter

PoS(ICRC2021)572

1. Introduction

The nature of the astronomical dark matter (DM), one of the main constituents of the Universe, is still under debate. A plethora of candidates have been proposed, among which one of the favoured possibilities is a weakly interacting and massive particle dubbed WIMP. If DM has been discovered only through the gravitational imprints it leaves on the dynamics of galaxies and galactic clusters, the WIMP hypothesis can be tested more directly. If they couple to ordinary matter, WIMPs should be produced at colliders and leave a signature in the final state in terms of missing energy. WIMPs can also collide on atoms inside a terrestrial detector and transfer energy to the recoiled nuclei and electrons. Yet another possibility is provided by the products left by the ongoing annihilations or decays of WIMPs in the Galaxy, among which high-energy photons, neutrinos and charged cosmic rays. Looking for an abnormal emission of these species allows to probe indirectly for the presence of WIMPs in the cosmos.

We will concentrate here on antimatter particles of the cosmic radiation, i.e. cosmic-ray (CR) positrons and antiprotons. These species are scarce since antimatter does not exist in the Universe after its primordial annihilation with matter. Today, antimatter is produced in trace amounts by the collisions of high-energy protons and helium nuclei on interstellar gas. Any excess againts these low backgrounds is a potential signal for WIMP dark matter. In that context, modeling correctly how charged particles propagate throughout the Galaxy is of paramount importance. Sec. 2 is devoted to that problem and to how we have derived CR propagation parameters, measuring in particular the height L of the magnetic halo [1, 2].

This height controls the fluxes of antimatter species produced by DM annihilation or decay. The more precise the determination of L, the more accurate the predictions of the DM-induced antimatter CR signal. A convenient way to bracket these predictions is to introduce the benchmark CR propagation models MIN, MED and MAX that yield minimal, median and maximal fluxes. These benchmarks were originally introduced in [3] for antiprotons and in [4] for positrons. They were included in public tools for DM searches, such as MICROMEGAS [5] or PPPC4DMID [6]. However, as a consequence of the plethora of increasingly precise CR data, they are now outdated. In Sec. 3, we explain how we derive the new benchmarks from the latest CR measurements [7]. Equipped with these new models, examples of DM antimatter CR signals are given in Sec. 4. We finally conclude in Sec. 5 where we discuss how we have improved upon previous analyses.

2. Measuring the height L of the magnetic halo

We use an advection-diffusion model where CR species propagate inside an infinite 1D magnetic halo with half-height L. The motion of the particles inside the turbulent magnetic fields of the Galaxy is phenomenologically described as a diffusion process with homogeneous but rigidity-dependent coefficient

$$K(R) = \beta^\eta K_0 \left\{ 1 + \left(\frac{R}{R_\mathrm{l}} \right)^{\frac{\delta_\mathrm{l} - \delta}{s_\mathrm{l}}} \right\}^{s_\mathrm{l}} \left\{ \frac{R}{1\,\mathrm{GV}} \right\}^{\delta} \left\{ 1 + \left(\frac{R}{R_\mathrm{h}} \right)^{\frac{\delta - \delta_\mathrm{h}}{s_\mathrm{h}}} \right\}^{-s_\mathrm{h}}, \tag{1}$$

where R denotes CR rigidity. From a few GV up to a few hundreds of GV, the spectral index of the diffusion coefficient in the inertial regime is δ while its normalization is set by K_0. A break

at $R_h \simeq 250$ GV needs to be introduced to explain the hardening of the primary CR fluxes. The three high-rigidity break parameters (R_h, δ_h, s_h) are set to the values reported in [8]. Below R_l, the index δ is replaced by δ_l to account for the spectral break seen in CR data below a few GV. This low-rigidity break can result from Galactic advection with vertical wind V_c, supplemented by diffusive reacceleration triggered by the Aflvénic speed V_a, or from damping effects in the magnetic turbulence spectrum on small scales. In [8], three CR transport schemes were introduced. The most general scheme is BIG with 7 free parameters $(K_0, \delta, R_l, \delta_l, V_c, V_a, L)$ while s_l is set to 0.05 for fast transition and $\eta = 1$. The configuration SLIM is a special case of BIG, with $V_a = V_c = 0$, and it has 5 free parameters $(K_0, \delta, R_l, \delta_l, L)$. The configuration QUAINT is also a special case of BIG with no low-rigidity break but a low-velocity tuning parameterised by η, and it has 6 free parameters $(K_0, \delta, \eta, V_c, V_a, L)$. We will be mostly concerned here with the SLIM scheme.

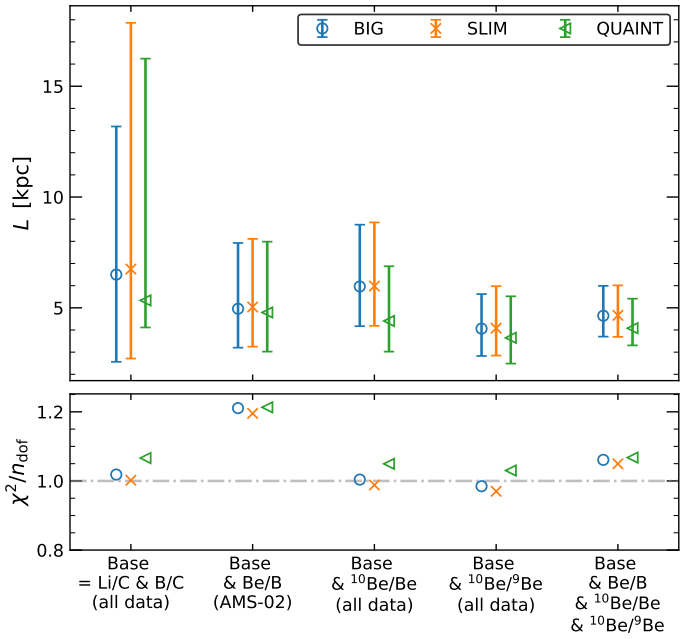

Figure 1: Best-fit halo size and asymmetric uncertainties for the BIG, SLIM and QUAINT schemes. From left to right, several data combinations are used. The first column ('Base') involves AMS-02 and low-energy B/C and Li/C data. The second column is the constraint set from AMS-02 data only (Li/C, B/C and Be/B). The remaining columns combine 'Base' data (from first column) to ^{10}Be/Be low-energy data (third column), to ^{10}Be/^{9}Be low- and intermediate-energy (next-to-last column), or combine all the previous cases (last column). For more details, see [1, 2].

At high energy, the abundance of secondary nuclei relative to their primay progenitors is proportional to L/K. At first order, the B/C and Li/C ratios cannot break the degeneracy between the diffusion coefficient K and the height L of the magnetic halo. On the contrary, unstable secondary species with lifetimes shorter than the escape time from the magnetic halo decay before experiencing its boundaries. These species are only sensitive to diffusion, hence the possibility to lift the degeneracy between K and L and to measure the vertical extension of the magnetic halo. One of the best candidates for this task is ^{10}Be whose half-lifetime $t_{1/2}$ is 1.387 Myr and related ratios ^{10}Be/^{9}Be and ^{10}Be/Be. However, most of the data available are at a few hundreds of MeV/n and are sensitive to Solar modulation. One way out of this difficulty is to use the complementary

AMS-02 Be/B high-precision data set covering the interval from ∼ 3 GV to ∼ 2 TV. In Fig. 1, we show how combining these various data sets allows to bracket down the uncertainty on L.

Using all these observations together, we fit [7] the CR propagation parameters within a 2D model via a chi-squared minimisation including nuisance terms for the nuclear cross sections and Solar modulation (treated within the force-field approximation). This minimisation is performed with the MINUIT package [9]. Its MINOS algorithm provides accurate asymmetric error bars even if the problem is very non-linear. We checked that the covariance matrix of uncertainties which we derive in the SLIM scheme without nuisance terms is in excellent agreement with the results of a Markov chain Monte Carlo analysis. The results of the full MINUIT analysis are showed in Tab. 1. In particular, the determination at the 2σ level of the magnetic halo height is $L = 4.66^{+2.94}_{-1.80}$ kpc.

$\log_{10} L$ [kpc]	δ	$\log_{10} K_0$ [kpc^2 Myr^{-1}]	R_1 [GV]	δ_1
0.668	0.499	−1.444	4.482	−1.110
+1.13e-2	−2.05e-4	+1.10e-2	+1.96e-3	+2.41e-3
−2.05e-4	+1.06e-4	−3.91e-4	+1.03e-6	−3.38e-4
+1.10e-2	−3.91e-4	+1.12e-2	+1.79e-3	+3.28e-3
+1.96e-3	+1.03e-6	+1.79e-3	+2.80e-2	+1.42e-2
+2.41e-3	−3.38e-4	+3.28e-3	+1.42e-2	+1.88e-2

Table 1: Cosmic ray parameter values and associated covariance matrix for the SLIM scheme.

3. Defining the new MIN, MED and MAX models

The DM signal is produced all over the magnetic halo and not solely inside the Galactic disk. It is approximately proportional to the ratio L^2/K where the diffusion coefficient is taken at the rigidity of interest. From a few GV upward, B/C and Li/C data constrain the ratio L/K so that the DM signal is merely proportional to L. The thicker the magnetic halo, the stronger the signal. At lower rigidities, L and K become independent. The more negative the low-energy index δ_1, the larger K at sub-GeV energies and the weaker the antiproton and positron fluxes. The CR parameters that crucially control the intensity of the DM signal are L and δ_1.

From the best-fit values and covariance matrix of Tab. 1, we draw a collection of 10^5 SLIM (correlated) propagation parameters. This sample is displayed in the (L, δ_1) plot of Fig. 2. Each blue point stands for a particular model within the SLIM propagation scheme. The constellation of dots is nearly circular, indicating that the CR parameters $\log_{10} L$ and δ_1 are not correlated with each other.

To define the MAX (resp. MIN) configuration, we start selecting a sub-sample of SLIM models whose quantiles relative to $\log_{10} L$ and to δ_1 are both larger (resp. smaller) than a critical value of

$$q^{\rm MAX}_{\rm MIN} = \frac{1}{2}\left(1 \pm {\rm erf}\left(\frac{n}{\sqrt{2}}\right)\right) \quad \text{where} \quad {\rm erf}(x) = 2/\sqrt{\pi}\int_0^x e^{-t^2}{\rm d}t\,. \tag{2}$$

Along each of the directions $\log_{10} L$ and δ_1, these models are located at more than n standard deviations from the average configuration. We have checked with the results presented in the next

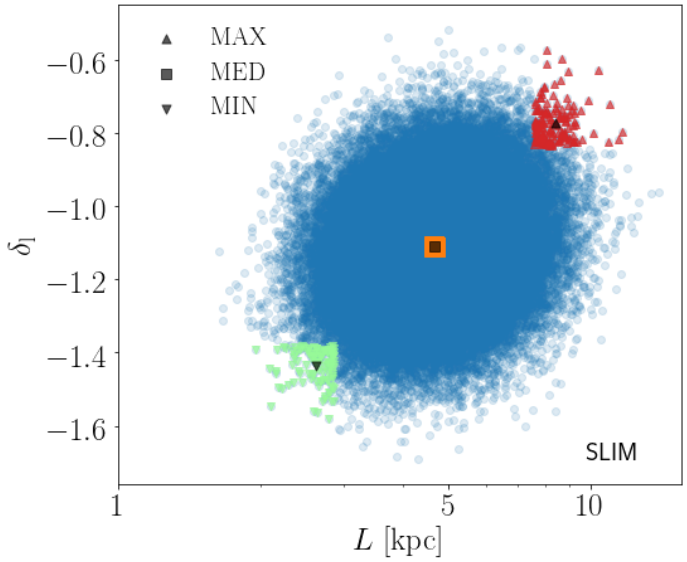

Figure 2: The constellation of blue dots features a sample of 10^5 randomly drawn SLIM models. Along each of the directions $\log_{10} L$ and δ_l, the red and green models are located at more than 2 standard deviations from the mean. The barycenters of these populations, defined with respect to all CR parameters, respectively yield the MAX and MIN configurations, depicted by the upward and downward black triangles. The MED model corresponds to the barycenter of the orange sub-sample.

section that a value of $n = 2$ defines MAX (resp. MIN) as a conservative two sigmas upper (res. lower) bound on the DM-produced primary fluxes, for any annihilation channel that we consider. In Fig. 2, this sub-sample corresponds to the red dots lying in the upper-right corner (resp. green points in the lower-left corner) of the blue constellation.

For the MED model, we proceed slightly differently. The orange square in Fig. 2 corresponds to a sub-sample of models whose quantiles relative to $\log_{10} L$ and to δ_l are both in the range extending from $q_{\rm MED} - p/2$ to $q_{\rm MED} + p/2$, with $q_{\rm MED} = 0.5$ and $p = 0.03$ a width parameter. Once that population is selected, the MED model corresponds once again to its barycentric configuration in the multi-dimensional space of all CR parameters. It is shown as a black square lying at the center of the orange square. The above-mentioned procedure leads to the CR parameters of Tab. 2.

SLIM	L [kpc]	δ	$\log_{10} K_0$ [kpc^2 Myr^{-1}]	R_l [GV]	δ_l
MAX	8.40	0.490	-1.18	4.74	-0.776
MED	4.67	0.499	-1.44	4.48	-1.11
MIN	2.56	0.509	-1.71	4.21	-1.45

Table 2: Propagation parameters for the MIN, MED, and MAX benchmarks of the SLIM scheme.

4. New MIN-MED-MAX fluxes on selected examples

In Fig. 3, we present examples of DM-generated antimatter fluxes. The primary positron (left) and antiproton (right) fluxes are calculated for a subset of the SLIM models derived in Sec. 3 and

a DM mass of 100 GeV. The positron flux is calculated using the so-called pinching method in a 2D setup [10], which is the most up-to-date semi-analytical procedure to incorporate all CR transport processes. The DM halo profile is borrowed from [11] with a galacto-centric distance $R_\odot$ of 8.21 kpc, a local DM density $\rho_\odot$ of 0.383 GeV cm^{-3} and a scale radius r_s set to 18.6 kpc.

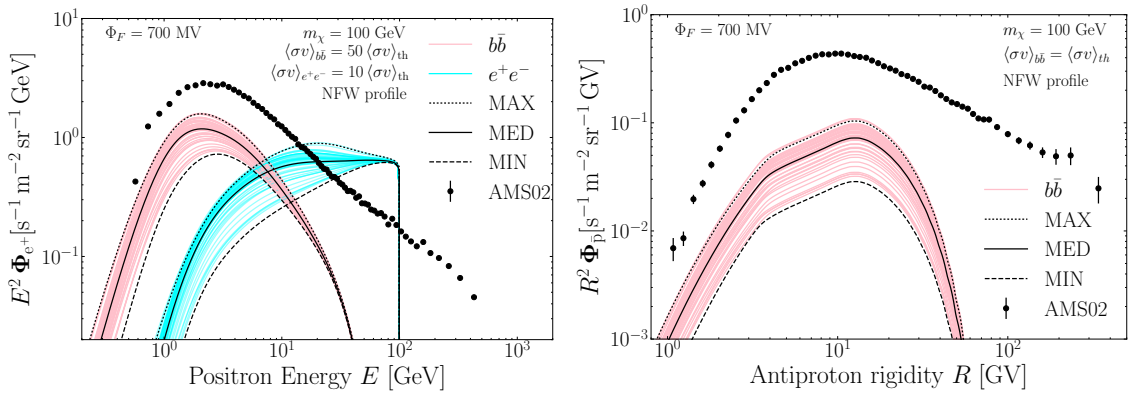

Figure 3: In the **left panel**, the primary positron fluxes are plotted as a function of positron energy for two different annihilation channels, i.e. $b\bar{b}$ in pink and e^+e^- in blue. The annihilation cross section has been respectively set to 1.5×10^{-24} and 3×10^{-25} cm^3 s^{-1}, to obtain primary fluxes roughly at the same level as the AMS-02 data [12], just for illustration purposes. The **right panel** features the antiproton yield for the same DM species and $b\bar{b}$ channel as above, with thermal annihilation cross section. For each channel, 50 CR models have been randomly selected and drawn in color. The MIN, MED, and MAX configurations respectively correspond to the dashed, solid and dotted black curves. All fluxes are modulated, with a Fisk potential of $\Phi_F = 700$ MV.

For positrons, we first notice that whatever the CR model, the predictions for a given annihilation channel converge to the same value at high energy. When the positron energy E is close to the DM mass, energy losses take over diffusion and positron production becomes local. It is no longer impacted by diffusion nor the magnetic halo boundaries. Moving towards smaller positron energies, the various curves separate from each other while keeping their respective positions down to approximately 1 GeV. At even lower energies, they are intertwined with one another and the high-energy ordering of the primary fluxes is lost. In the case of the SLIM parametrization, the low-energy index δ_1 of the diffusion coefficient comes into play and redistributes the fluxes in the sub-GeV range. However, because the MIN, MED, and MAX models (represented by the black lines) have actually been selected from both L and δ_1, they do *not* exhibit that trend and the corresponding fluxes follow the expected hierarchy. In particular, the extreme MIN (dashed) and MAX (dotted) curves nicely encapsulate the bulk of flux predictions down to the lowest energies. Although they have been derived from CR parameters alone, the MIN and MAX configurations can thus be used to determine the range over which primary positron fluxes are expected to lie.

In the right panel of Fig. 3, the antiproton flux is derived for the same $b\bar{b}$ channel as for the positrons, but here with a thermal annihilation cross section of 3×10^{-26} cm^3 s^{-1}. This time, diffusion alone dominates over the other CR transport processes. Consequently, whatever the energy, the antiproton flux scales like L^2/K as explained in Sec. 3. We notice that the pink curves, which can be considered as a representative sample of all possible antiproton flux predictions, are once again contained within the band delineated by the MIN (dashed) and MAX (dotted) lines. The

width of this band is furthermore independent of energy and corresponds to a factor of ~ 4.

5. Bracketing down uncertainties

The MIN, MED, and MAX models allow to gauge the uncertainty arising from CR propagation. As the precision of CR measurements has been considerably improving in the past decade, so has the accuracy of the theoretical predictions. This trend is clear in Fig. 4 where several uncertainty bands are featured for the $b\bar{b}$ and e^+e^- channels. In the case of the $b\bar{b}$ channel for instance, the new uncertainty bands from 1 GV to 10 GV are reduced by a factor of 3-4 (positrons) and 5 (antiprotons) with respect to their initial version [3, 4].

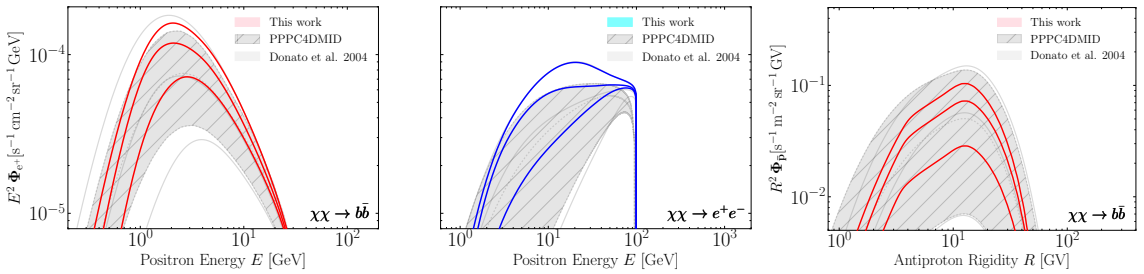

Figure 4: The theoretical uncertainty on primary fluxes owing to CR propagation has been shrinking as a result of more accurate measurements. The light-gray bands correspond to the original determination of the MIN, MED, and MAX models by [3] for antiprotons and by [4] for positrons. The hatched-gray regions feature the slightly improved predictions proposed in the framework of PPPC4DMID by [13] for antiprotons and [14] for positrons. The results of this work [7] are illustrated in the SLIM case by the pink ($b\bar{b}$ channel) and blue (e^+e^-) strips, for positrons (left and middle panel) and for antiprotons (right panel). They point toward an improvement of how DM induced fluxes are now calculated.

In this analysis, we have derived new MIN, MED, and MAX benchmark parameter sets that correspond to the minimal, median, and maximal fluxes of DM-produced antimatter CRs in the Galaxy, as allowed by constraints set by standard CRs. They replace their former version, previously used in the literature for antiprotons and positrons. The new derived parameters are actually valid for both species, and for light anti-nuclei more generally. The benchmarks corresponding to the QUAINT and BIG schemes are also given in [7]. The BIG scheme retains the full complexity of the transport process, with little approximations, while the QUAINT scheme puts the stress on reacceleration and convection.

In practice, the DM practitioner interested in estimating, in an economical and effective way, the variability of DM CR fluxes induced by Galactic propagation can use the SLIM MIN-MED-MAX sets. For a more complete analysis, the user can also rely on the BIG and QUAINT benchmarks. Going beyond the MIN-MED-MAX references can also be achieved in more involved analyses using the covariance matrices of the propagation parameters, as provided for instance in Tab. 1 for SLIM.

To conclude, our revised CR benchmarks lead to a significant reduction of the uncertainty band. Hence any new DM analysis employing these new sets can be expected to reduce the uncertainty of the DM properties (most notably the constraints on the annihilation cross section or the decay rate) in the same proportions.

References

[1] N. Weinrich, Y. Génolini, M. Boudaud, L. Derome and D. Maurin, *Combined analysis of AMS-02 (Li,Be,B)/C, N/O, ^{3}He, and ^{4}He data*, *A&A* **639** (2020) A131 [2002.11406].

[2] N. Weinrich, M. Boudaud, L. Derome, Y. Génolini, J. Lavalle, D. Maurin et al., *Galactic halo size in the light of recent AMS-02 data*, *A&A* **639** (2020) A74 [2004.00441].

[3] F. Donato, N. Fornengo, D. Maurin, P. Salati and R. Taillet, *Antiprotons in cosmic rays from neutralino annihilation*, *Phys. Rev. D* **69** (2004) 063501 [astro-ph/0306207].

[4] T. Delahaye, R. Lineros, F. Donato, N. Fornengo and P. Salati, *Positrons from dark matter annihilation in the galactic halo: Theoretical uncertainties*, *Phys. Rev. D* **77** (2008) 063527 [0712.2312].

[5] G. Bélanger, F. Boudjema, P. Brun, A. Pukhov, S. Rosier-Lees, P. Salati et al., *Indirect search for dark matter with micrOMEGAs_2.4*, *Computer Physics Communications* **182** (2011) 842 [1004.1092].

[6] M. Cirelli, G. Corcella, A. Hektor, G. Hütsi, M. Kadastik, P. Panci et al., *PPPC 4 DM ID: a poor particle physicist cookbook for dark matter indirect detection*, *J. Cosmology Astropart. Phys.* **3** (2011) 51 [1012.4515].

[7] Y. Génolini, M. Boudaud, M. Cirelli, L. Derome, J. Lavalle, D. Maurin et al., *New minimal, median, and maximal propagation models for dark matter searches with galactic cosmic rays*, 2103.04108.

[8] Y. Génolini, M. Boudaud, P. Ivo Batista, S. Caroff, L. Derome, J. Lavalle et al., *Cosmic-ray transport from AMS-02 B/C data: benchmark models and interpretation*, *Phys. Rev. D* **99** (2019) 123028 [1904.08917].

[9] F. James and M. Roos, *Minuit - a system for function minimization and analysis of the parameter errors and correlations*, *Computer Physics Communications* **10** (1975) 343.

[10] M. Boudaud, E.F. Bueno, S. Caroff, Y. Genolini, V. Poulin, V. Poireau et al., *The pinching method for Galactic cosmic ray positrons: Implications in the light of precision measurements*, *A&A* **605** (2017) A17 [1612.03924].

[11] P.J. McMillan, *The mass distribution and gravitational potential of the Milky Way*, *MNRAS* **465** (2017) 76 [1608.00971].

[12] AMS Collaboration et al., *Towards Understanding the Origin of Cosmic-Ray Positrons*, *Phys. Rev. Lett.* **122** (2019) 041102.

[13] M. Boudaud, M. Cirelli, G. Giesen and P. Salati, *A fussy revisitation of antiprotons as a tool for Dark Matter searches*, *JCAP* **05** (2015) 013 [1412.5696].

[14] J. Buch, M. Cirelli, G. Giesen and M. Taoso, *PPPC 4 DM secondary: A Poor Particle Physicist Cookbook for secondary radiation from Dark Matter*, *JCAP* **09** (2015) 037 [1505.01049].